Amino Acids (2013) 45:327–338
DOI 10.1007/s00726-013-1503-3

ORIGINAL ARTICLE

Small molecules interacting with α-synuclein: antiaggregating and cytoprotective properties

Anna Marchiani · Stefano Mammi · Giuliano Siligardi · Rohanah Hussain · Isabella Tessari · Luigi Bubacco · Giovanna Delogu · Davide Fabbri · Maria A. Dettori · Daniele Sanna · Sonia Dedola · Pier A. Serra · Paolo Ruzza

Received: 24 January 2013 / Accepted: 19 April 2013 / Published online: 5 May 2013

Abstract Curcumin, a dietary polyphenol, has shown a potential to act on the symptoms of neurodegenerative disorders, including Alzheimer's and Parkinson's diseases, as a consequence of its antioxidant, anti-inflammatory and anti-protein aggregation properties. Unfortunately, curcumin undergoes rapid degradation at physiological pH into ferulic acid, vanillin and dehydrozingerone, making it an unlikely drug candidate. Here, we evaluated the ability of some curcumin by-products: dehydrozingerone (**1**), its *O*-methyl derivative (**2**), zingerone (**3**), and their biphenyl analogues (**4–6**) to interact with α-synuclein (AS), using CD and fluorescence spectroscopy. In addition, the antioxidant properties and the cytoprotective effects in rat pheochromocytoma (PC12) cells prior to intoxication with H_2O_2, MPP+ and $MnCl_2$ were examined while the Congo red assay was used to evaluate the ability of these compounds to prevent aggregation of AS. We found that the biphenyl zingerone analogue (**6**) interacts with high affinity with AS and also displays the best antioxidant properties while the biphenyl analogues of dehydrozingerone (**4**) and of *O*-methyl-dehydrozingerone (**5**) are able to partially inhibit the aggregation process of AS, suggesting the potential role of a hydroxylated biphenyl scaffold in the design of AS aggregation inhibitors.

Keywords α-Synuclein · Biphenyl compounds · Curcumin-like molecules · Parkinson's disease · Protein aggregation

A. Marchiani · S. Mammi · P. Ruzza (✉)
Padua Unit, Institute of Biomolecular Chemistry of CNR, Padua, Italy
e-mail: paolo.ruzza@unipd.it

A. Marchiani · S. Mammi
Department of Chemical Sciences, University of Padua, Padua, Italy

G. Siligardi · R. Hussain
Diamond Light Source Ltd., Rutherford Appleton Laboratory, Chilton, Didcot, Oxfordshire OX11 0QX, UK

I. Tessari · L. Bubacco
Department of Biology, University of Padua, Padua, Italy

G. Delogu · D. Fabbri · M. A. Dettori · D. Sanna
Sassari Unit, Institute of Biomolecular Chemistry of CNR, Sassari, Italy

S. Dedola · P. A. Serra
Department of Clinical and Experimental Medicine, Medical School, University of Sassari, Sassari, Italy

Introduction

Parkinson's disease (PD) belongs to the group of protein misfolding diseases (PMD). The hallmark of these pathologies is the aggregation and accumulation of specific misfolded proteins (Naiki and Nagai 2009). PD is characterized by the progressive degeneration of the dopaminergic neurons from the substantia nigra of the brain. The processes underlying dopaminergic cell death remain unclear. Among others, two biochemical mechanisms have been proposed for the pathogenesis of PD that are relevant to the present study: (1) the intracellular accumulation and aggregation of misfolded proteins, such as α-synuclein (AS) and parkin, which constitute the core of Lewy bodies; (2) oxidative stress caused by reactive metabolites of dopamine and alterations in the levels of iron and glutathione in the substantia nigra accompany this mitochondrial dysfunction (Hauser and Hastings 2013; Oueslati et al. 2010; Roth 2009).

In this framework, a main goal in exploring therapeutic approaches for PD is the design of small molecules that can simultaneously target two of these processes (e.g., aggregation and oxidative stress, or aggregation and metal ions). Recent experimental findings indicate that various antioxidants, including polyphenols, have potent anti-fibrillogenic effects and destabilize AS fibrils in in vitro models (Ono and Yamada 2006; Wang et al. 2010). Specifically, the presence of 4-substituted-2-methoxy phenols seems to be an important structural and functional requirement for biological activity (Priyadarsini et al. 1998). Within this class of compounds, curcumin, the principal curcuminoid present in the curry spice turmeric, has recently been shown to interact with AS reducing its cytotoxicity in a Parkinson's disease cell model (Wang et al. 2010). Curcumin also possesses potent antioxidant and anti-inflammatory properties and the ability to counteract numerous neurodegenerative processes such as apoptosis, mitochondrial dysfunction, microglial activation and protein aggregation. Unfortunately, curcumin has poor bioavailability due to its low solubility in aqueous solution and its rapid degradation at physiological pH into ferulic acid, vanillin and dehydrozingerone (Fig. 1) (Wang et al. 1997).

Dehydrozingerone exhibits a potent anti-inflammatory activity in various models and scavenges oxygen radicals such as hydroxyl and superoxide anion (Parihar et al. 2007; Liu et al. 2008).

Here, we examined the ability of dehydrozingerone (**1**), (Fig. 2), its *O*-methyl derivative (**2**), zingerone (**3**), and their C-2 symmetric dimers (biphenyls **4–6**, respectively) to interact with AS and to modulate its aggregation process, using biophysical techniques such as fluorescence, circular dichroism (CD) and synchrotron radiation circular dichroism (SRCD). These results were compared with their antioxidant and neuroprotective activity. We found that the biphenyl zingerone analogue (**6**) interacts with high affinity with AS and also displays the best antioxidant properties while the biphenyl analogues **4** and **5** are able to partially inhibit the aggregation process of AS. These results suggest that a hydroxylated biphenyl scaffold may be used as a useful tool to develop compounds which are able to prevent the aggregation of AS and also possess antioxidant properties that may inhibit post translational modifications of AS caused by oxidative stress. It is well known that reactive oxygen/nitrogen species (ROS/RNS) react with susceptible amino acid residues of AS, inducing methionine oxidation, tyrosine nitration and dimer formation that were shown to promote the formation of oligomeric intermediates of AS (Schildknecht et al. 2013; Xiang et al. 2013).

Experimental procedures

Chemistry

Unless otherwise stated, starting materials, reagents and solvents were obtained from commercial suppliers and were used without further purification. Acetone was freshly distilled from $CaCl_2$. Melting points were determined on a Büchi 530 apparatus (Assago, Italy) and are uncorrected. Unless otherwise specified all ^{1}H- and ^{13}C-NMR spectra were recorded in $CDCl_3$ with a Varian Mercury Plus (Palo Alto, CA) spectrometer at 400 and 100.57 MHz, respectively. Chemical shifts are given in ppm (δ); multiplicities are indicated by s (singlet), d (doublet) or dd (doublet of doublets). Elemental analyses were performed using a Perkin-Elmer model 240 C elemental analyser (Waltham, Massachusetts). Flash chromatography was carried out with silica gel 60, 230–400 mesh (Aldrich, Milano, Italy) eluting with appropriate solution in the stated v:v proportions. Analytical TLC was performed with either 0.25-mm thick silica gel plates (Polygram Sil G/UV254, Macherey–

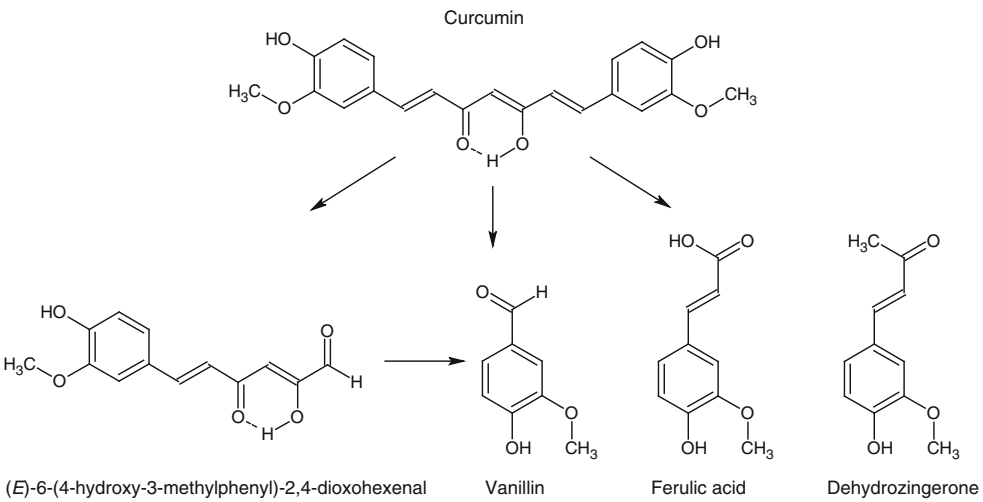

Fig. 1 Degradation by-products of curcumin

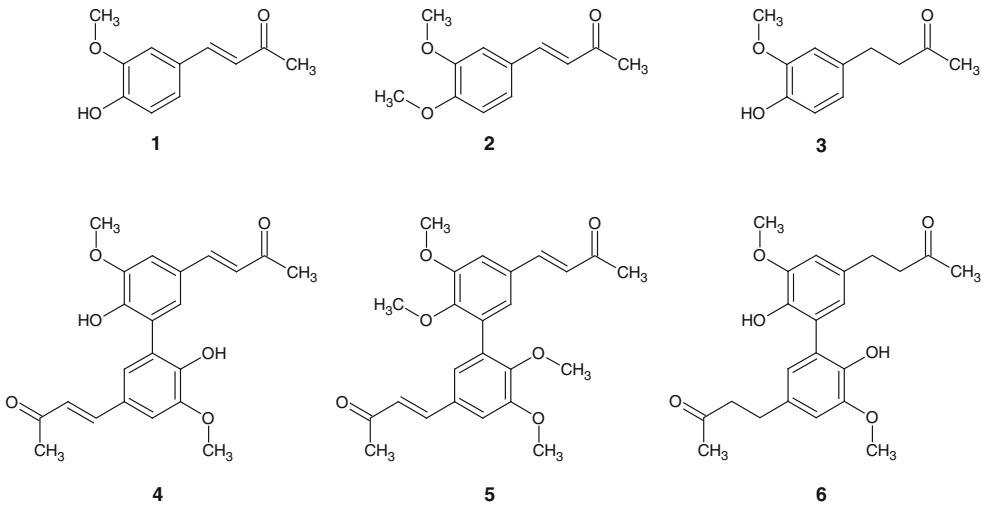

Fig. 2 Structure of dehydrozingerone (**1**), *O*-methyldehydrozingerone (**2**) and zingerone (**3**), and their biphenyl dimers (**4–6**)

Nagel, VWR International, Milano Italy) or 0.2-mm thick silica gel plates (60 F254 Merck, Milano, Italy). The purity of all new compounds was judged to be >98 % by ^{1}H-NMR and ^{13}C-NMR.

Dehydrozingerone [(*E*)-4-(4-hydroxy-3-methoxyphenyl)but-3-en-2-one] (**1**)

To a stirred solution of vanillin (1.50 g, 9.8 mmol) in acetone (50 mL) at room temperature and under N_2, an aqueous solution (1 N) of NaOH (30 mL, 30.0 mmol) was added dropwise. The mixture was stirred at room temperature for 12 h. The solvent was roto-evaporated and water and 10 % HCl were cautiously added. The heterogeneous solution was extracted with ether, dried over Na_2SO_4 and evaporated to afford a brown solid. The crude material was purified by flash chromatography using of CH_2Cl_2 as eluent, to give **1** (1.69 g, 90 %): mp 126–127 °C [lit. 127–128 °C (Elias and Rao 1988)]. ^{1}H NMR δ ppm 2.38 (s, 3H), 3.85 (s, 3H), 5.96 (bs, 1H), 6.53 (d, $J = 16.0$ Hz, 1H), 6.92 (d, $J = 8.0$ Hz, Ar, 1H), 7.04 (d, $J = 1.6$ Hz, Ar, 1H), 7.01 (dd, $J = 1.6$, 8.0 Hz, Ar, 1H), 7.42 (d, $J = 16.0$ Hz, 1H); ^{13}C NMR δ ppm 27.29, 56.93, 109.28, 114.81, 123.95, 124.98, 126.90, 143.77, 146.88, 148.26, 198.46; Anal. Calcd for $C_{11}H_{12}O_3$: C, 68.74; H, 6.29; Found: C, 68.90; H, 6.40.

O-Methyl-dehydrozingerone [(*E*)-4-(3,4-dimethoxyphenyl)but-3-en-2-one] (**2**)

To a solution of **1** (0.40 g, 2.1 mmol) and K_2CO_3 (0.32 g, 2.3 mmol) in dry acetone (20 mL), CH_3I (0.33 g, 2.3 mmol) was added dropwise at room temperature under N_2. The solution was stirred at reflux for 12 h. Acetone was roto-evaporated and water and 10 % HCl were cautiously added. The solution was extracted with ether, dried over Na_2SO_4 and evaporated to afford a yellow solid. The crude material was purified by flash chromatography using a 1:3 mixture of ethyl acetate:petroleum ether as eluent. (0.39 g, 92 %): mp 86–87 °C [lit. 85–87 °C (Narender and Reddy 2007)]. ^{1}H NMR δ ppm 2.37 (s, 3H), 3.91 (s, 6H), 6.59 (d, $J = 16.0$ Hz, 1H), 6.87 (d, $J = 8.4$ Hz, Ar, 1H), 7.06 (d, $J = 2.0$ Hz, Ar, 1H), 7.11 (dd, $J = 2,8$ Hz, Ar, 1H), 7.45 (d, $J = 16.0$ Hz, 1H); ^{13}C NMR δ ppm 27.34, 55.89, 55.98, 109.61, 111.08, 122.99, 125.26, 127.33, 143.49, 149.29, 151.36, 198.31; Anal. Calcd for $C_{12}H_{14}O_3$: C, 60.88; H, 6.84; Found: C, 60.79; H, 6.71.

Dehydrodivanillin [6,6′-dihydroxy-5,5′-dimethoxy-[1,1′-biphenyl]-3,3′-dicarbaldehyde]

To a solution of vanillin (10.64 g, 70 mmol) in 700 mL of water, $FeSO_4$ heptahydrate (0.4 g, 1.4 mmol) was added at room temperature (Delomenede et al. 2008). The solution was stirred for 10 min at 50 °C and $Na_2S_2O_8$ (8.93 g, 33.0 mmol) was added. The reaction mixture was stirred at 50 °C for 5 days. The brown precipitate formed was filtered off. The solid was dissolved in an aqueous NaOH (10 %) solution. Aqueous HCl (10 %) solution was added and the brown precipitate was filtered. (10 g, 95 %); mp >270 °C. ^{1}H NMR (DMSO-*d6*) δ ppm: 3.94 (s, 6H); 7.42 (s, 4H); 9.80 (s, 2H); 9.89 (s, 2H). ^{13}C NMR (DMSO-*d6*) δ ppm: 56.50, 109.70, 125.18, 128.23, 128.62, 148.60, 150.90, 191.60; Anal. Calcd for $C_{16}H_{14}O_6$: C, 63.57; H, 4.67; Found: C, 63.60; H, 4.49.

Dehydrozingerone dimer [(3*E*,3′*E*)-4,4′-(6,6′-dihydroxy-5,5′-dimethoxy-[1,1′-biphenyl]-3,3′-diyl)bis(but-3-en-2-one)] (**4**)

To a stirred solution of dehydrodivanillin (2.00 g, 6.6 mmol) in acetone (50 mL) at room temperature and

under N_2, an aqueous solution (1 N) of LiOH (40 mL, 40.0 mmol) was added dropwise. The mixture was stirred at reflux for 12 h. Water and 10 % HCl were cautiously added. The precipitate was filtered, washed with water and dried to afford a yellow solid. (2.10 g, 83 %): mp 242–243 °C. ^{1}H NMR δ ppm 2.36 (s, 6H), 3.98 (s, 6H), 5.30 (bs, 2H), 6.60 (d, $J = 16.0$ Hz, 2H), 7.1 (d, $J = 2.0$ Hz, Ar, 2H), 7.14 (d, $J = 2.0$ Hz, Ar, 2H), 7.47 (d, $J = 16.0$ Hz, 2H); ^{13}C NMR δ ppm 27.32, 56.22, 108.77, 123.57, 125.27, 125.44, 126.60, 143.51, 145.45, 147.36, 198.30; Anal. Calcd for $C_{22}H_{22}O_6$: C, 69.10; H, 5.80; Found: C, 69.49; H, 5.74.

O-Methyl-dehydrozingerone dimer (**5**)

The synthesis of this compound has been described by Pisano et al. (2010). ^{1}H NMR δ ppm 2.35 (s, 6H), 3.69 (s, 6H), 3.95 (s, 6H), 6.63 (d, $J = 16.4$ Hz, 2H), 7.05 (d, $J = 2.0$ Hz, Ar, 2H), 7.11 (d, $J = 2.0$ Hz, Ar, 2H), 7.45 (d, $J = 16.4$ Hz, 2H); ^{13}C NMR δ ppm 27.46, 55.91, 60.85, 110.80, 124.10, 126.47, 129.82, 132.32, 143.04, 149.05, 153.02, 198.22; Anal. Calcd for $C_{24}H_{26}O_6$: C, 70.23; H, 6.38; Found: C, 69.89; H, 6.48.

Zingerone dimer [4,4′-(6,6′-dihydroxy-5,5′-dimethoxy-[1,1′-biphenyl]-3,3′-diyl)bis(butan-2-one)] (**6**)

To a solution of **3** (1.58 g, 8.0 mmol) in dry dichloromethane (15 mL), a solution of methyl-tributylammonium permanganate (MTBAP) (1.30 g, 4.00 mmol) (Marques et al. 1998) in dry dichloromethane (15 mL) was added dropwise at room temperature under N_2. The solution was stirred at room temperature for 1 h and then washed with an aqueous solution of $Na_2S_2O_5$ (50 mL) The organic layer was separated, washed with water, dried over Na_2SO_4 and evaporated to afford a white solid that was purified by flash chromatography using a 1:2 mixture of ethyl acetate:petroleum ether as eluent. (0.99 g, 65 %): mp 85–86 °C. ^{1}H NMR δ ppm 2.14 (s, 6H), 2.74–2.88 (series of m, 8 h), 3.90 (s, 6H), 6.01 (bs, 2H), 6.71 (d, $J = 2.0$ Hz, 2H), 6.73 (d, $J = 2.0$ Hz, Ar, 2H); ^{13}C NMR δ ppm 29.50, 30.13, 45.46, 56.09, 110.64, 122.68, 124.38, 132.88, 140.90, 147.18, 208.11; Anal. Calcd for $C_{22}H_{26}O_6$: C, 68.38; H, 6.78; Found: C, 69.49; H, 5.74.

Expression of AS

α-Synuclein was expressed in *Escherichia coli* strain BL21(DE3) from a pET-28 plasmid according to the procedure described by Huang et al. (2005). The AS concentration was determined by absorption spectroscopy ($\varepsilon = 5{,}960$ M^{-1} cm^{-1} at 280 nm).

Fluorescence measurements

Fluorescence spectra were recorded from 285 to 385 nm using a Perkin-Elmer LS50B spectrofluorimeter, with the excitation and emission slit widths set at 5 nm. The excitation wavelength was 275 nm.

The following procedure was used for the titration of AS with compounds **1**–**6**: 900 μL of AS solution (3.0 μM in 10 mM Tris–HCl buffer, pH 6.8) was placed in a quartz cell (1.0 cm pathlength) and small amounts of the ligand stock solution (3 mM in EtOH) were added to achieve ligand/AS molar ratios from 0 to 40. The ethanol added with the ligand never exceeded 5 % v/v.

Circular dichroism

All measurements were performed at 25 °C using a nitrogen-flushed Chirascan-Plus Circular Dichroism Spectrometer (Applied Photophysics, Surrey, UK) using a 0.1-cm quartz cell. The CD spectra were recorded using a bandwidth of 1 nm and the data presented is the average of four scans. AS was dissolved in 20 mM phosphate buffer, pH 6.8 while ligands were dissolved in 4:6 v/v EtOH–phosphate buffer. Ligand concentrations were determined by absorption spectroscopy.

Aggregation studies

A 100-μM solution of AS in 20 mM phosphate buffer, pH 6.8 was prepared and added with 0.03 % NaN_3 to avoid any bacterial growth. The solution was filtered through a 0.1-μm filter to remove any aggregated material. The compounds to be tested were dissolved in ethanol and added to the protein solution to achieve a final concentration of 200 μM in a total volume of 1 mL. Ethanol never exceeded 8 % of the volume. Each sample was then incubated in an Eppendorf Thermomixer Compact (Hamburg, Germany) at 37 °C and 500 rpm for 12 days. From each sample, small aliquots were taken at different times and analyzed through UV–Vis studies with Congo red (CR) as a probe. For each sample at different times, 18-μL aliquots were taken and added to a solution of 20 μM CR in 20 mM phosphate buffer, pH 6.8 to achieve a final CR/protein ratio equal to 5:1 and the absorption spectrum was immediately collected from 650 to 400 nm at 25 °C, bandwidth 1 nm, with a 1-cm pathlength quartz cell (Hellma, Ltd.). The spectra were measured using a LAMBDA 950 UV/Vis/NIR Perkin-Elmer spectrophotometer. For each analysis, the spectrum of CR alone was measured before adding the aliquots. SRCD spectra from 180 to 260 nm were collected at the beamline B23 module end station B, with bandwidth of 1.2 nm, integration time of 1 s, 1 nm digital resolution, 39 nm/min scan speed, and

two repeated scan per spectrum, using Suprasil cells (Hellma Ltd.) with 0.1 cm pathlength. Samples were diluted with buffer to obtain a theoretical protein concentration of 5 μM.

Free-radical scavenging capacity

EPR measurements were carried out at room temperature using a Bruker EMX spectrometer (Bruker BioSpin GmbH, Rheinstetten, Germany) operating at the X-band (9.4 GHz) equipped with a quartz flat cell. EPR instrument settings were: field center, 3,460 G; sweep width, 100 G; modulation amplitude, 1 G; microwave power, 20 mW (10 dB); receiver gain, 5×10^5. For each sample, at least two spectra were recorded.

For the quantification of the DPPH concentration present in each sample, double integration is required since the spectra were measured as second derivative of the absorption. A careful examination of the EPR spectra shows that the linewidth is the same in all the samples, that is, there is no variation in the linewidth changing the DPPH concentration. For this reason, instead of doubly integrating, the height of the central line was taken as a measure of the intensity of the signals.

For TEAC (Trolox Equivalent Antioxidant Capacity) assay, ABTS [2,2′-azino-bis(3-ethylbenzthiazoline-6-sulphonic acid)] was dissolved in water to obtain a final concentration of 7 mM. The ABTS radical cation ($ABTS^{\cdot+}$) was produced by reacting an ABTS stock solution with potassium peroxodisulfate (final concentration 2.45 mM) and allowing the mixture to stand in the dark at room temperature overnight before use. To measure the antioxidant capacity of compounds **1–6** and for the reference compound Trolox, the $ABTS^{\cdot+}$ solution was diluted with ethanol to an absorbance of ca. 0.70 at 750 nm. Stock solutions of compounds **1–6** were diluted such that, after introduction of a 10-μL aliquot of each dilution into the assay, they produced 20–80 % reduction of the blank absorbance. After addition of 1.0 mL of the diluted $ABTS^{\cdot+}$ solution to 10 μL of compounds **1–6** in dichloromethane or Trolox standard in ethanol (final concentration 0–15 μM), the absorbance reading was taken exactly 6 min after mixing. Appropriate solvent blanks were run in each assay. Experiments were performed on a Perkin-Elmer model Lambda 35 spectrophotometer at room temperature. All determinations were carried out in triplicate.

Cell viability

Hydrogen peroxide and 1-methyl-4-phenylpyridinium (MPP+) were purchased from Sigma-Aldrich (Milan, Italy), manganese chloride from Merck (Darmstadt, Germany), curcumin (purity of 95 %) from Alfa Aesar (GmbH & Co KG, Karlsruhe, Germany). Stock H_2O_2 (5 mM) and $MnCl_2$ (25 mM) solutions were prepared in Milli-Q water and diluted (20–100 μM, or 0.2–1 mM, respectively) in complete medium. MPP+ solutions (25 mM) were prepared in PBS and diluted (0.2–1 mM) in complete medium. Curcumin and curcumin-like derivative solutions (100 mM) were prepared in DMSO and then diluted to the final concentration in complete medium, containing a concentration of DMSO <0.1 %. All solutions were prepared immediately before use. All experiments were performed on PC12 cells during their exponential phase of growth. Cells were maintained at 37 °C in 100 mm plastic culture plates in a humidified atmosphere of 5 % CO_2—95 % air in a Dulbecco's modified Eagle's medium (DMEM)-F12 supplemented with 10 % horse serum and 5 % foetal calf serum. For each experiment, 50×10^3 cells/cm^2 were plated and treated 24 h later (time 0). To study the potential protective effects of curcumin and curcumin-like derivatives, PC12 cells were preincubated for 20 min with each antioxidant molecule and then exposed to increasing concentrations of H_2O_2, MPP+ and $MnCl_2$ for 24 h obtaining cell mortality around 40 %. In preliminary experiments, we determined the lowest protective concentration of curcumin (40 μM) against the above-indicated toxics, which was used in all subsequent experiments with curcumin-like compounds done in triplicate. Cell viability was evaluated by means of the MTT [3-(4,5-dimethylthiazol-2-yl)-2,5-diphenyltetrazolium bromide] method (Mosmann 1983) with minor modifications. The absorbance at 578 nm was measured by means of a Bauty Diagnostic microplate reader within 1 h. The percentage of cell survival was calculated from the absorbance values as follows:

$$[(A_{\text{tested}} - A_{\text{blank}})/(A_{\text{untreated}} - A_{\text{blank}}) \times 100]$$

with A_{blank} referring to the absorbance of wells that contained only the medium and MTT.

Results and discussion

Chemical synthesis

The synthesis of dehydrozingerone (**1**) and of its methyl ether (**2**) is depicted in Scheme 1. The Claisen-Schmidt condensation of vanillin with acetone in the presence of aqueous NaOH (3 eq.), overnight at room temperature, followed by acidification of the reaction mixture using HCl to induce dehydration, gave compound **1** in quantitative yield. *O*-Methylation of **1** with methyl iodide in acetone provided compound **2**. Zingerone (**3**) is commercially available, and was used without any further purification steps.

Scheme 1 Synthesis of compounds **1** and **2**

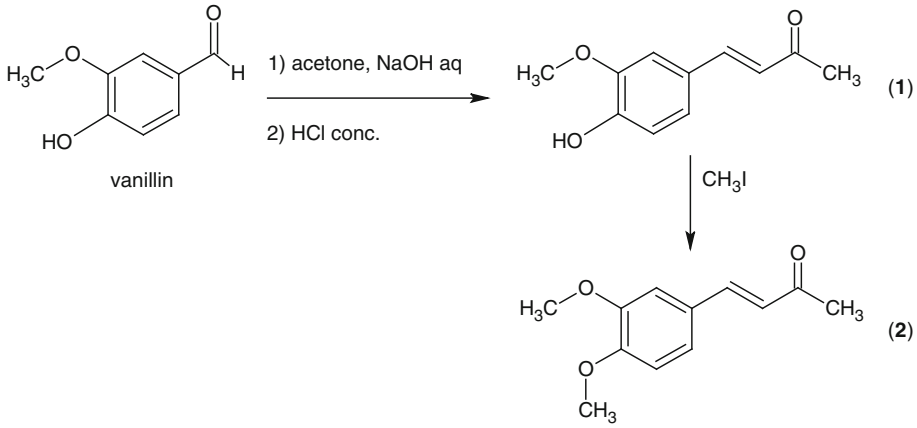

The synthesis of the biphenyl analogue of zingerone (**6**) was achieved following a previously described procedure (Delogu et al. 2000). Compound **6** was prepared in 65 % yield by C–C coupling of **3** in the presence of methyltributylammonium permanganate (MTBAP) in dichloromethane at room temperature for 1 h (Scheme 2a). Unfortunately, this procedure was unsuccessful in the preparation of dimers **4** and **5**.

Compound **4** was synthesized by Claisen–Schmidt condensation of dehydrodivanillin with acetone in the presence of a large excess of aqueous LiOH overnight at room temperature, followed by acidification with HCl (83 % yield) (Scheme 2b). The *O,O'*-dimethyl analogue **5** was synthesized by quantitative reaction of **4** with methyl iodide in acetone (Pisano et al. 2010).

α-Synuclein interaction

The interaction of compounds **1–6** with AS was investigated by both CD and fluorescence spectroscopies. The far-UV CD spectrum of AS in the absence of ligand displayed a negative band at about 195 nm (Fig. 3), characteristic of the essentially unstructured nature of AS in aqueous environment. After the addition of ligands (compounds **1–6**), we observed only a small changes in the intensity of the negative band at 195 nm, indicating the absence of a folded AS conformation induced by the interaction with compounds **1–6**.

The apparent dissociation constant ($K_d = 1/K_a$) values of the AS-ligand complexes (Table 1) were determined by fluorescence spectroscopy. AS contains four tyrosine residues (Y39, Y125, Y133, Y136), which were used as endogenous fluorescence probes. The addition of increasing amounts of ligand quenched the tyrosine fluorescence of AS. The relative fluorescence Tyr emission (e.g. compound **3** in Fig. 4) was corrected for the inner filter effect according to the procedure described by Montalti et al. (2006) and the apparent association constant (K_a) values as well as the number of binding sites (n) were determined from the following equation (Jiang et al. 2004)

$$\log \frac{F_0 - F}{F} = \log K_a + n \log[\text{ligand}]$$

where F and F_0 represent the observed and initial fluorescence values, respectively.

Zingerone (**3**) shows a tighter interaction with AS than dehydrozingerone derivatives **1** and **2**, which may be due to the higher flexibility of the aliphatic side chain. The dimerization process increases the affinity towards AS with the following affinity order: the biphenyl analogue of zingerone (**6**) binds with the highest affinity, but the dimer of *O*-methyl-dehydrozingerone (**5**) interacts with an affinity fourfold higher than the dimer of dehydrozingerone (**4**). Each compound binds with a 1:1 stoichiometry with the exception of compounds **4** and **5** that show an n value of 1.41 and 1.33, respectively.

α-Synuclein aggregation

The ability of compounds **1–6** to interfere with AS aggregation was evaluated using the Congo red assay. This dye strongly interacts with amyloid aggregates, showing both an increase in intensity and a red shift of the absorption band. Although Congo red partially inhibits fibril formation, its use in single time-point experiments is well established (Howie and Brewer 2009). A freshly prepared solutions of AS (100 μM) was portioned in seven different vials, AS alone as control and in the presence of 2.5 eq. of compounds **1–6**, which were incubated with shaking at 37 °C. Aliquots of these samples were taken at different times and the absorption spectra in the 400–650 nm region were acquired immediately after the addition of a Congo red solution (Fig. 5).

After 2 days of incubation at 37 °C, a peak at about 540 nm, increasing in a time-dependent manner, appears in the absorption spectra, indicative of the interaction of Congo red with soluble amyloid fibrils.

Scheme 2 Synthesis of biphenyl dimers **4–6**

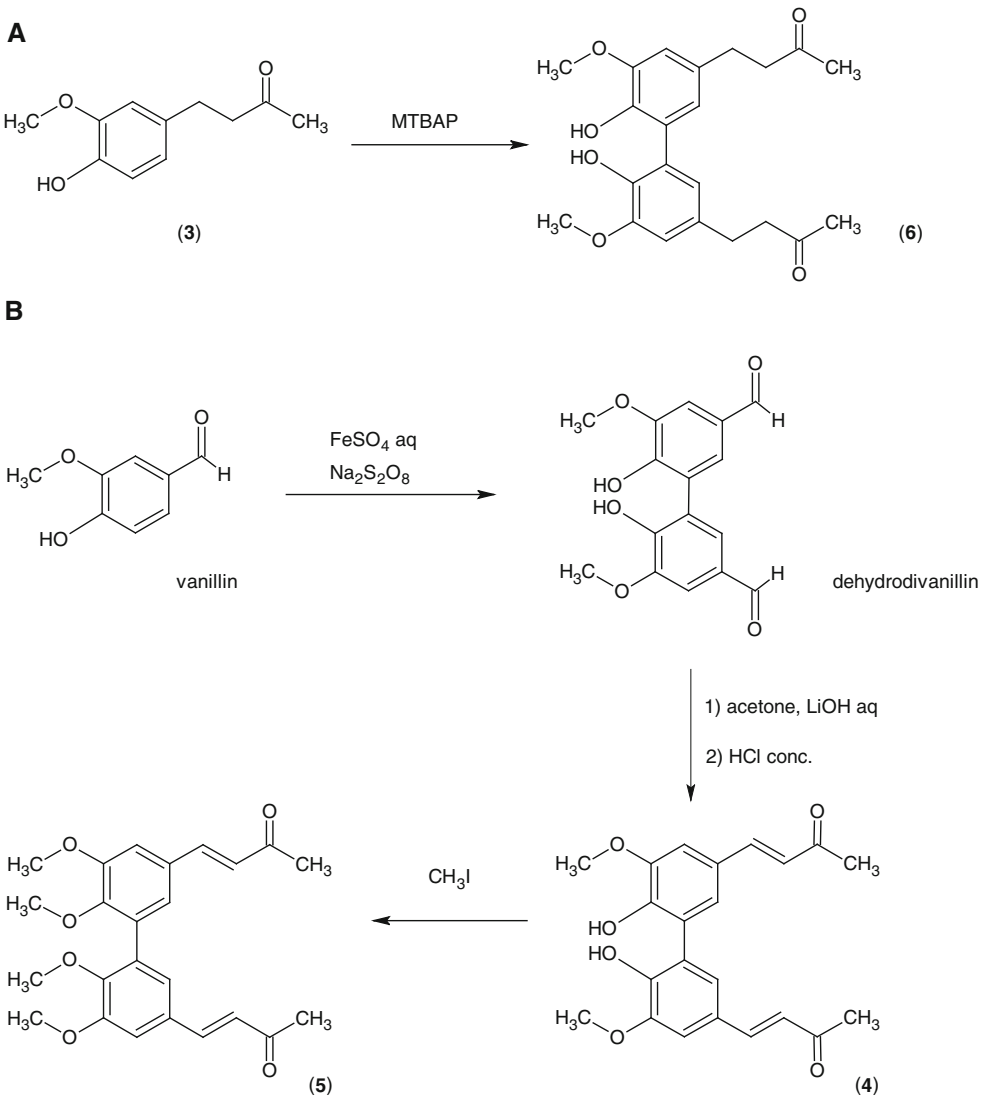

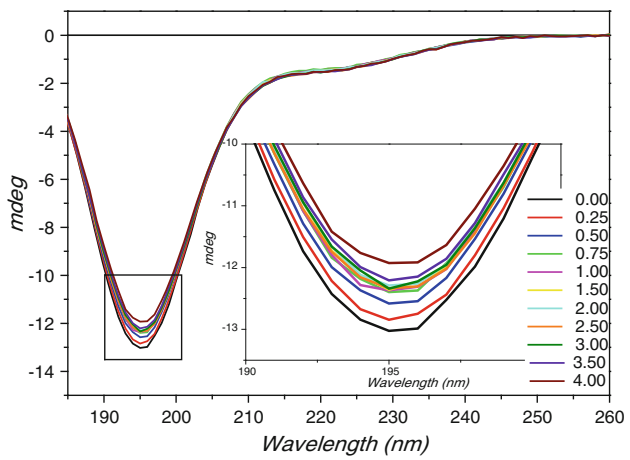

Fig. 3 Far-UV CD spectra of AS in the presence of increasing amounts of compound **3** (indicated). AS concentration was 5 μM in 20 mM phosphate buffer, pH 6.8; compound **3** stock concentration was either 100 or 200 μM in ethanol–phosphate buffer (4:6, v/v). Spectra were recorded at 25 °C (color figure online)

Table 1 K_d values and number of binding sites (n) of each AS-ligand complex

Compound	K_d (μM)	n
1	13.10	0.97
2	25.60	1.07
3	5.20	1.09
4	2.62	1.41
5	0.66	1.33
6	0.11	1.03

The difference absorbance values at 538 nm of Congo red in the presence of AS alone or with inhibitors are plotted against time in Fig. 6. The trend of absorbance values is different between the protein alone and in the presence of compounds **1–6**, suggesting an alteration of the aggregation process of AS due to small organic molecules. In particular, in the presence of compounds **4** and **5**, the

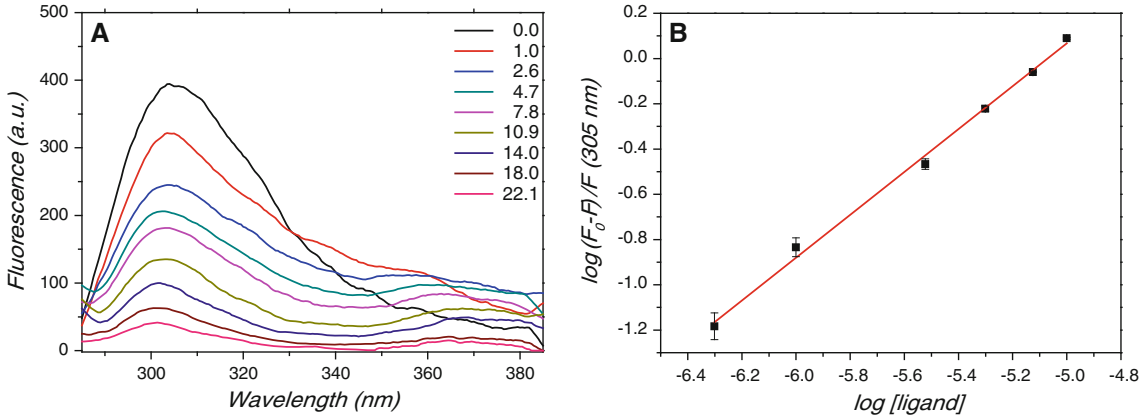

Fig. 4 AS tyrosine fluorescence quenching at increasing amounts of compound **3**. **a** Fluorescence spectra were measured as a function of the increasing ligand/AS molar ratios (indicated). AS was 3 μM in 10 mM Tris-HCl buffer, pH 6.8; compound **3** stock concentration was 200 μM in ethanol–phosphate buffer (4:6, v/v). Spectra were recorded at 25 °C. **b** Logarithmic plots of fluorescence quenching of AS treated with different ligand concentrations. The parameters plotted on the two axes are described in the text (color figure online)

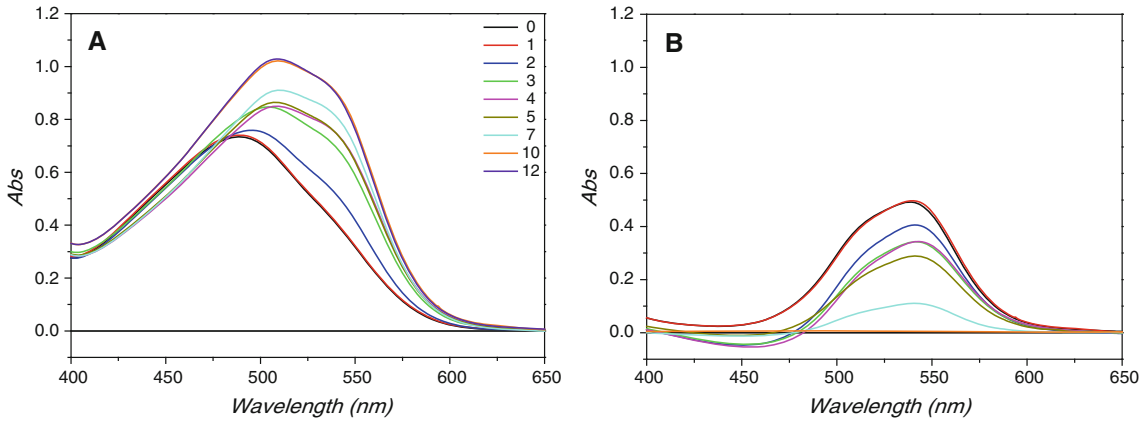

Fig. 5 Congo red assay of AS aggregation. **a** Visible absorption spectra of Congo red in the presence of AS solution at different times of incubation (days, indicated). **b** Difference absorption spectra of Congo red obtained by subtraction of the spectrum recorded at time zero (color figure online)

Congo red absorbance values at 12 days are about half that of AS alone, indicating a reduced amount of AS amyloid fibrils in the sample. To confirm this result, the secondary structures of AS alone and in the presence of compounds **4** and **5**, at the end of the aggregation experiment, were evaluated by SRCD. The far-UV SRCD spectrum of AS in the absence of ligand and after 12 days of incubation displayed a negative maximum at about 217 nm and a positive maximum at about 195 nm, characteristic of the presence of a β-sheet structure (Fig. 7). However, the far-UV SRCD spectra of AS incubated in the presence of compound **4** or **5** and recorded in the same conditions are characterized by the presence of a broad negative band that may be deconvoluted into two bands centered at about 220 and 195–200 nm. These bands have the same intensities in the presence of compound **4** while the band at 220 nm is predominant in the solution incubated with compound **5**. These spectra resemble that described for AS in the presence of baicalein, a flavonoid able to inhibit AS fibrillation via the stabilization of specific oligomers that possess a relatively well-developed secondary structure (Hong et al. 2008).

Antioxidant activity

The antioxidant capacity of compounds **1–6** was assessed by both DPPH and TEAC assays (Brand-Williams et al. 1995; Re et al. 1999). The DPPH scavenging assay was conducted using EPR spectroscopy. The characteristic EPR spectrum of the DPPH radical (a quintet with hyperfine splitting of 8.7 G) is reported in Fig. 8. The addition of increasing amounts of a selected compound (e.g. compound **4**) to the control reduced the intensity of the DPPH signal.

The central peak of each spectrum was used to quantify the relative amount of DPPH present in a given sample. The results demonstrated that each compound reduced the DPPH signal in a concentration-dependent manner. The free-radical scavenging activity of compounds **1–6** is

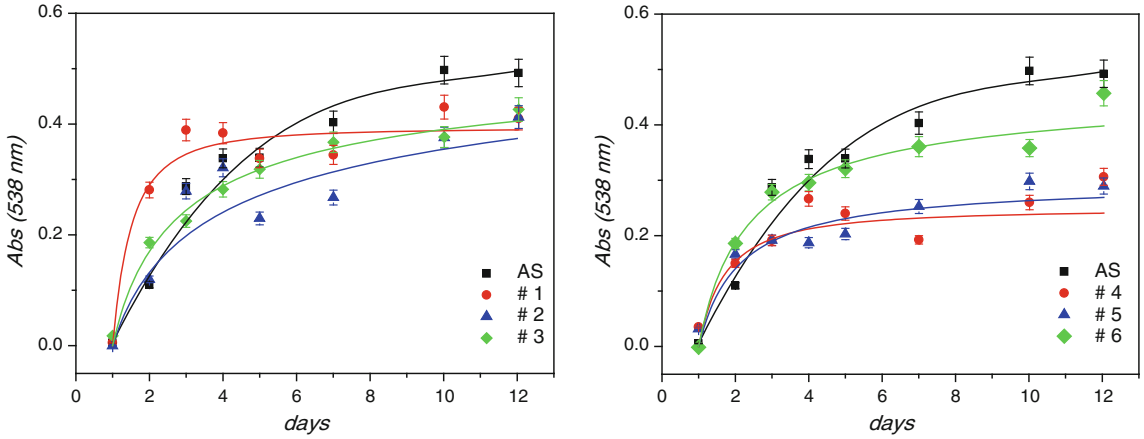

Fig. 6 Difference absorbance values at 538 nm of Congo red in the presence of AS alone or with inhibitors (indicated) incubated for different times (color figure online)

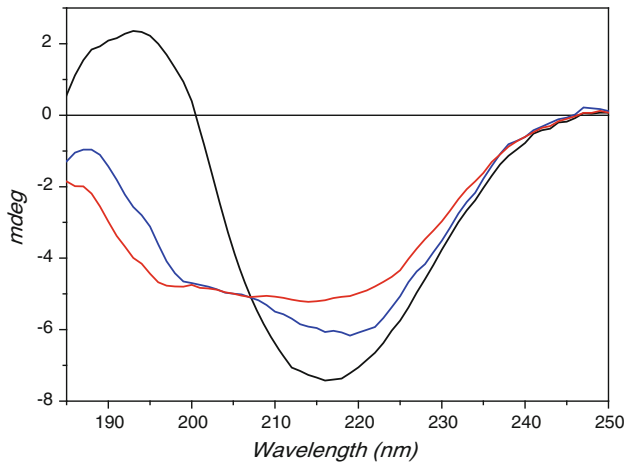

Fig. 7 Far-UV SRCD spectra of AS alone (*black line*) or in the presence of 2.5 equiv. of compounds **4** (*red line*) or **5** (*blue line*) after 12 days of incubation at 37 °C (color figure online)

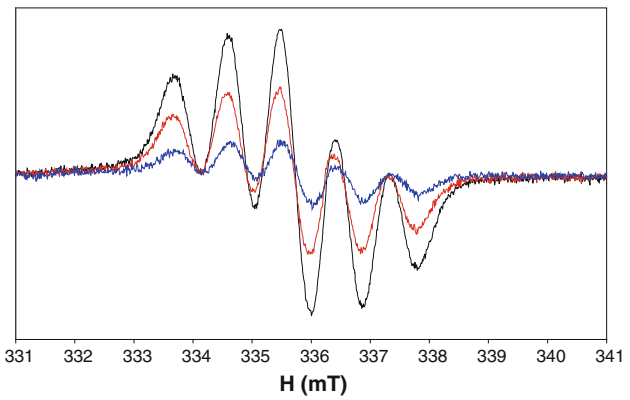

Fig. 8 Typical EPR spectra of a 50-μM ethanol solution of DPPH radical in the absence (*black*) or in the presence of different amounts of compound **4**: 16 μM (*red*) and 32 μM (*blue*) (color figure online)

Table 2 Antioxidant capacity of compounds **1–6** measured with DPPH and TEAC assays

Compound	*DPPH* IC_{50} (μM)	TEAC[a]
1	54.8	1.274
2	5620.0	0.001
3	25.1	1.122
4[b]	35.2	1.235
5[b]	2000.0	0.015
6[b]	22.8	1.829

[a] Expressed as [Trolox]/[compound]

[b] For the DPPH assay, the concentration is expressed as phenolic group

expressed as IC_{50} (Table 1). The antioxidant capacity was also evaluated using the TEAC assay. This test measures the capacity in terms of Trolox equivalents necessary to reduce the ABTS radical cation previously produced. The data reported in Table 1 indicate that compounds **2** and **5**, having no hydroxyl groups that may contribute to scavenge the DPPH radical, exhibit much lower activity than the other compounds. These results are consistent with published data since flavonoids and other phenolic compounds act as radical scavengers due to the presence of the phenolic moiety. Dimers of **1** and **3** show a different behaviour with respect to the corresponding monomer in the DPPH assay. As shown in Table 2, the IC_{50} value of **4** is significantly lower than that of the parent compound **1**, while **3** and **6** show comparable IC_{50} values.

In the TEAC assay, compounds **2** and **5** show much lower values than those measured for the other compounds in agreement with the results of the DPPH assay. The

highest TEAC value is shown by compound **6** while compounds **1**, **3** and **4** displayed comparable values. The intermediate order of these compounds is not the same in the two tests, but it is generally believed that the mechanism of the DPPH assay is hydrogen atom transfer while the TEAC assay proceeds via electron transfer; therefore, these assay report on different processes.

A question remains about the structural feature primarily responsible for the antioxidant activity: is it the dimeric form or the buten-3-en-2-one/butan-2-one side chain? Table 2 indicates compounds **6** and **3** as ranking first and second for antioxidant capacity and the TEAC test confirms the ranking of compound **6**, suggesting that the dimeric structure is primarily responsible for the antioxidant activity while the butan-2-one side chain is more suited to determine the antioxidant properties than the buten-3-en-2-one. This superior radical scavenging activity of biphenyl structures has been confirmed by Witting et al. (1996) who analyzed over 60 antioxidant compounds including biphenyl derivatives of natural and synthetic (poly)phenols.

Neuroprotective activity

The in vitro neuroprotective activity of compounds **1–6** was evaluated analyzing cell death induced by H_2O_2, MPP+ and $MnCl_2$ in rat pheochromocytoma (PC12) cells. This cell line is a good model to study oxidative stress associated with PD (Siddiqui et al. 2011). In particular, MPP+ induced both apoptotic and necrotic PC12 cell death, and increased the expression of a 57-kDa species of AS. This species of AS, larger than the monomer, has been reported to be an oligomer or an aggregated form of the protein (Xu et al. 2007). The survival of the PC12 cells was assessed by the MTT assay described in Methods. Control cell groups were cultured under the standard conditions described above, with no additional treatment. H_2O_2, MPP+ and $MnCl_2$ treatment groups were incubated in H_2O_2 (75 μM), MPP+ (0.5 mM) and $MnCl_2$ (0.75 mM) for a duration of 24 h before assays were performed. The effects of compounds **1–6** were assessed by the addition of these molecules to a final concentration of 40 μM, which corresponds to the lowest protective concentration of curcumin against the toxics indicated above.

The assessment of cell survival by the MTT reduction method is shown in Fig. 9. All values are expressed as percentage of the control (no treatment) group. Cell viability at 24 h after exposure to H_2O_2, MPP+ and $MnCl_2$ was reduced, respectively, to 55, 64 and 54 % of the control values.

As shown in Fig. 9, the viability of PC12 cells was significantly reduced by exposure to compounds **2** (81 %), **4** (80 %) and **5** (12 %) compared with controls. Dose–response studies (data not shown) confirmed the cytotoxicity of these compounds. Specifically, compound **5** significantly reduced cell viability already at the concentration of 10 μM (65 %) while compound **2** shows a slight toxicity at 20-μM concentrations. In the whole range of concentrations tested (from 10 to 80 μM), compounds **2**, **4** and **5** do not protect cells from the analyzed insults (Fig. 9).

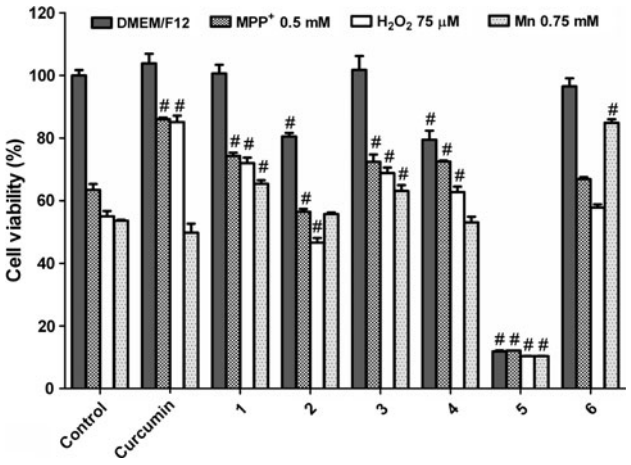

Fig. 9 Effects of curcumin or dehydrozingerone-like compounds **1–6** (40 μM) on the viability of PC12 cells in culture medium alone (DMEM/F12) or supplemented with H_2O_2 (75 μM), MPP+ (0.5 mM) or $MnCl_2$ (0.75 mM). $^{\#}P < 0.05$ versus the corresponding control

Conversely, compounds **1** and **3** provide a statistically significant protection from the insults analyzed. Surprisingly, compound **6** protected cells only against $MnCl_2$ damage.

Curcumin significantly protected cells from H_2O_2 and MPP+ toxic effects while it failed to protect cells exposed to $MnCl_2$. These results suggest that minor differences in molecule design result in drastic differences in toxicity/neuroprotection on PC12 cells alone or exposed to toxic compounds. This observation suggests that mechanisms of these effects are diverse and appear to involve actions on various molecular targets (Zhou et al. 2011).

Conclusions

In an effort to evaluate new small bifunctional molecules **1–6** as lead compounds for innovative therapeutic approaches in PD, we found that curcumin-like compounds **1** and **3** exhibited good radical scavenging capacity and neuroprotective activity in PC12 cells, but they are both poor AS ligands and unable to inhibit AS aggregation. On the contrary, their biphenyl derivatives interacted with high affinity with AS. In particular, compound **6** showed the highest affinity towards AS, as well as the highest antioxidant capacity in both DPPH and TEAC assays, and a protective effect against the toxic effect of $MnCl_2$ on PC12

cells; unfortunately, it did not interfere with the aggregation process of AS. Compound **4** was able to partially inhibit the aggregation process of AS, but it offered only limited protection to PC12 cells. The properties of compounds **2** and **5** make them unsuitable molecules for both their poor activity as antioxidant and their high cytotoxicity toward PC12 cells.

In summary, the data presented in this article suggests the utility of a hydroxylated biphenyl scaffold as the basis for the design of new AS amyloid fibril inhibitors. Previously, Baures et al. (1998) demonstrated that biphenyl analogues were effective in vitro inhibitors of transthyretin fibrillation. This assumption is highly relevant in light of the recent results of Bartels et al. (2011) demonstrating that monomeric AS represents the least abundant species in normal cells, and that the predominant physiological species of AS in cells and brain is a helical folded tetramer, like transthyretin.

Acknowledgments This work was supported by Sardinia Autonomous Region, L.R. 7th August 2007, no. 7; and by FIRB-MERIT Program "Molecular bases in ageing-related degenerative syndromes" (RBNE08HWLZ).

Conflict of interest The authors declare no competing financial interest.

References

Bartels T, Choi JG, Selkoe DJ (2011) alpha-Synuclein occurs physiologically as a helically folded tetramer that resists aggregation. Nature 477:107–111

Baures PW, Peterson SA, Kelly JW (1998) Discovering transthyretin amyloid fibril inhibitors by limited screening. Bioorg Med Chem 6:1389–1401

Brand-Williams W, Cuvelier ME, Berset C (1995) Use of a free radical method to evaluate antioxidant activity. LWT-Food Sci Technol. 28:25–30

Delogu G, Fabbri D, Dettori MA, Forni A, Casalone G (2000) Chiral nonracemic C2-symmetry biphenyls by desymmetrization of 6,6′,2,2′-tetramethoxy-1,1′-biphenyl. Tetrahedron Asymmetry 11:4417–4427

Delomenede M, Bedos-Belval F, Duran H, Vindis C, Baltas M, Negre-Salvayre A (2008) Development of novel antiatherogenic biaryls: design, synthesis, and reactivity. J Med Chem 51: 3171–3181

Elias G, Rao MNA (1988) Synthesis and anti-inflammatory activity of substituted (e)-4-phenyl-3-buten-2-ones. Eur J Med Chem 23: 379–380

Hauser DN, Hastings TG (2013) Mitochondrial dysfunction and oxidative stress in Parkinson's disease and monogenic parkinsonism. Neurobiol Dis 51:35–42

Hong DP, Fink AL, Uversky VN (2008) Structural characteristics of alpha-synuclein oligomers stabilized by the flavonoid baicalein. J Mol Biol 383:214–223

Howie AJ, Brewer DB (2009) Optical properties of amyloid stained by Congo red: history and mechanisms. Micron 40:285–301

Huang CJ, Ren GP, Zhou H, Wang CC (2005) A new method for purification of recombinant human alpha-synuclein in Escherichia coli. Protein Expr Purif 42:173–177

Jiang M, Xie MX, Zheng D, Liu Y, Li XY, Chen X (2004) Spectroscopic studies on the interaction of cinnamic acid and its hydroxyl derivatives with human serum albumin. J Mol Struct 692:71–80

Liu YZ, Dolence J, Ren J, Rao MNA, Sreejayan N (2008) Inhibitory effect of dehydrozingerone on vascular smooth muscle cell function. J Cardiovasc Pharmacol 52:422–429

Marques FA, Simonelli F, Oliveira ARM, Gohr GL, Leal PC (1998) Oxidative coupling of 4-substituted 2-methoxy phenols using methyltributylammonium permanganate in dichloromethane. Tetrahedron Lett 39:943–946

Montalti M, Credi A, Prodi L, Gandolfi MT (2006) Handbook of photochemistry. CRC Press, Taylor & Francis Group, Boca Raton, pp 561–600

Mosmann T (1983) Rapid colorimetric assay for cellular growth and survival: application to proliferation and cytotoxicity assays. J Immunol Methods 65:55–63

Naiki H, Nagai Y (2009) Molecular pathogenesis of protein misfolding diseases: pathological molecular environments versus quality control systems against misfolded proteins. J Biochem 146:751–756

Narender T, Reddy KP (2007) A simple and highly efficient method for the synthesis of chalcones by using borontrifluoride-etherate. Tetrahedron Lett 48:3177–3180

Ono K, Yamada M (2006) Antioxidant compounds have potent anti-fibrillogenic and fibril-destabilizing effects for alpha-synuclein fibrils in vitro. J Neurochem 97:105–115

Oueslati A, Fournier M, Lashuel HA (2010) Role of post-translational modifications in modulating the structure, function and toxicity of alpha-synuclein: implications for Parkinson's disease pathogenesis and therapies. In: Bjorklund A, Cenci M (eds) Recent Advances in Parkinsons Disease: Basic Research. Elsevier Science BV, Amsterdam, pp 115–145

Parihar VK, Dhawan J, Kumar S, Manjula SN, Subramanian G, Unnikrishnan MK, Rao CM (2007) Free radical scavenging and radioprotective activity of dehydrozingerone against whole body gamma irradiation in Swiss albino mice. Chem Biol Interact 170:49–58

Pisano M, Pagnan G, Dettori MA, Cossu S, Caffa I, Sassu I, Emionite L, Fabbri D, Cilli M, Pastorino F, Palmieri G, Delogu G, Ponzoni M, Rozzo C (2010) Enhanced anti-tumor activity of a new curcumin-related compound against melanoma and neuroblastoma cells. Mol Cancer 9:137–148

Priyadarsini KI, Guha SN, Rao MNA (1998) Physico-chemical properties and antioxidant activities of methoxy phenols. Free Radic Biol Med 24:933–941

Re R, Pellegrini N, Proteggente A, Pannala A, Yang M, Rice-Evans C (1999) Antioxidant activity applying an improved ABTS radical cation decolorization assay. Free Radic Biol Med 26:1231–1237

Roth J (2009) Are there common biochemical and molecular mechanisms controlling manganism and parkisonism. NeuroMol Med 11:281–296

Schildknecht S, Gerding HR, Karreman C, Drescher M, Lashuel HA, Outeiro TF, Di Monte DA, Leist M (2013) Oxidative and nitrative alpha-synuclein modifications and proteostatic stress: implications for disease mechanisms and interventions in synucleinopathies. J Neurochem. doi:10.1111/jnc.12226

Siddiqui MA, Kashyap MP, Kumar V, Tripathi VK, Khanna VK, Yadav S, Pant AB (2011) Differential protection of pre-, co- and post-treatment of curcumin against hydrogen peroxide in PC12 cells. Hum Exp Toxicol 30:192–198

Wang YJ, Pan MH, Cheng AL, Lin LI, Ho YS, Hsieh CY, Lin JK (1997) Stability of curcumin in buffer solutions and

characterization of its degradation products. J Pharm Biomed Anal 15:1867–1876

Wang MS, Boddapati S, Emadi S, Sierks MR (2010) Curcumin reduces alpha-synuclein induced cytotoxicity in Parkinson's disease cell model. BMC Neurosci 11:57

Witting PK, Westerlund C, Stocker R (1996) A rapid and simple screening test for potential inhibitors of tocopherol-mediated peroxidation of LDL lipids. J Lipid Res 37:853–867

Xiang W, Schlachetzki JC, Helling S, Bussmann JC, Berlinghof M, Schäffer TE, Marcus K, Winkler J, Klucken J, Becker CM (2013) Oxidative stress-induced posttranslational modifications of alpha-synuclein: specific modification of alpha-synuclein by 4-hydroxy-2-nonenal increases dopaminergic toxicity. Mol Cell Neurosci 54:71–83

Xu J, Wei CZ, Xu CQ, Bennett MC, Zhang GH, Li FC, Tao EX (2007) Rifampicin protects PC12 cells against MPP+-induced apoptosis and inhibits the expression of an alpha-Synuclein multimer. Brain Res 1139:220–225

Zhou HY, Beevers CS, Huang SL (2011) The Targets of Curcumin. Curr Drug Targets 12:332–347